

## Suppression of superconductivity in Mn-substituted MgCNi<sub>3</sub>

A. Das\* and R. K. Kremer

*Max-Planck-Institut für Festkörperforschung, 70569 Stuttgart, Germany*

(Received 21 March 2003; published 7 August 2003)

We report the effect of doping Mn in the isostructural MgCNi<sub>3-x</sub>Mn<sub>x</sub> ( $x=0-0.05$ ) compounds. Magnetic susceptibility, resistivity, magnetoresistance, and specific heat studies show evidence of localized moments and Kondo effect in samples with  $x \neq 0$ . The rapid suppression of superconductivity ( $\sim -21$  K/at.% Mn) in these compounds is a consequence of pair breaking effects due to moment formation on Mn.

DOI: 10.1103/PhysRevB.68.064503

PACS number(s): 74.70.Dd, 74.62.Dh, 72.15.Qm

### I. INTRODUCTION

The intermetallic compound MgCNi<sub>3</sub> has recently been reported to exhibit superconductivity with  $T_C \sim 8$  K.<sup>1</sup> It is related structurally to the borocarbides  $RT_2B_2C$  ( $T = \text{Ni, Pd}$ ) (Refs. 2,3) and may be viewed as three dimensional analogue of these from the point of arrangement of the Ni atoms. This structural relationship therefore, provides the possibility of comparing the properties between these two. MgCNi<sub>3</sub> has generated interest because of its simple perovskite structure and absence of a ferromagnetic ground state inspite of a large proportion of Ni per unit cell. The superconducting ground state has raised the question of the role of Ni-3d bands and led to the suggestion that MgCNi<sub>3</sub> to be a candidate for unconventional superconductivity.<sup>4</sup> Electronic structure calculations show Ni d-band derived density of states to dominate the electronic states at the Fermi energy  $E_F$ .<sup>5-8</sup> The Mg and C atoms provide a contribution to the electronic density of states (DOS) at about 1 eV below  $E_F$ . The proximity of the Ni d band to  $E_F$  may lead to spin fluctuations or magnetic order which could eventually suppress superconductivity. The absence of ferromagnetism in MgCNi<sub>3</sub> is shown to result from low values of the Stoner factor  $S=0.43$ ,<sup>6</sup> 0.64,<sup>7</sup> and the DOS. Similarly, absence of antiferromagnetism has been ruled out due to lack of nesting features at the Fermi surface.<sup>6</sup> The electronic structure calculations also indicate that doping at one of the three atomic sites could induce a large change in the superconducting state. In particular, electronic structure calculations predict that hole doping<sup>9</sup> could drive the system to a ferromagnetic ground state while electron doping<sup>8</sup> could lead to Fermi surface nesting and subsequently induce a charge density wave or spin density wave instability.

The nature of superconductivity in MgCNi<sub>3</sub> is far from being resolved, experimentally. MgCNi<sub>3</sub> crystallizes in the cubic perovskite structure with C atoms in the body center position surrounded by Ni atoms at the face center position, and Mg atoms at cube corners. The superconducting phase as determined from neutron diffraction experiments is found to be MgC<sub>0.96</sub>Ni<sub>3</sub> for  $T_C \sim 8$  K.<sup>1</sup> The sensitivity of the superconducting properties to the Mg and C content has been studied and it was found that  $T_C$  decreases systematically with decreasing C content.<sup>10,11</sup> Superconductivity is identified with the  $\beta$ -MgCNi<sub>3</sub> cubic phase with cell constant  $\sim 3.816$  Å.<sup>12</sup> The superconductivity is described within the

BCS model. However the strength of electron-phonon coupling reported varies from weak,<sup>13</sup> moderate,<sup>14</sup> to strong coupling.<sup>15,16</sup> NMR studies indicate that the nature of pairing to be s wave,<sup>17</sup> and Hall effect results show that the carriers are of electron type.<sup>13</sup> However, tunneling experiments indicate that MgCNi<sub>3</sub> is a strong coupling superconductor with non-s-wave pairing symmetry.<sup>15</sup>

There are a number of theoretical<sup>18-20</sup> and experimental<sup>21-23</sup> studies on the effect of doping at the Ni site in MgCNi<sub>3</sub>. Doping the Ni site with other transition metals leads to changes in the degree of filling of partially filled Ni d bands which influences the superconducting properties. Experimentally, effect of doping in MgCNi<sub>3-x</sub>T<sub>x</sub> ( $T = \text{Cu, Co, Fe, and Mn}$ ) is found to suppress superconductivity in varied ways. Substituting Ni by Cu (limited to 3% by the solubility of Cu into Ni) leads to a decrease of  $T_C$  from 7 to 6 K.<sup>21</sup> Hayward *et al.*<sup>21</sup> observe that doping with 1% Co suppresses bulk superconductivity. Resistivity measurements by Kumary *et al.*<sup>22</sup> and Ren *et al.*<sup>23</sup> on Co doped samples show that  $T_C$  systematically decreases from 7.7 to 7.1 K for  $x$  between 0 and 0.4. In the case of partially substituting Ni with Fe, it is found that  $T_C$  initially increases.<sup>22</sup> Magnetic ordering has not been reported in either Fe or Co substituted samples, in strong contrast to theoretical predictions. A Brief report on Mn substitution indicates that superconductivity is suppressed in samples with  $x=0.125$  and 0.5.<sup>23</sup> In this communication we present results which demonstrate that doping by Mn leads to suppression of superconductivity much more pronounced than previously observed. We identify, this behavior to be related with the formation of localized moments on Mn and a concomitant Kondo effect.

### II. EXPERIMENTAL DETAILS

In our study polycrystalline samples with nominal composition Mg<sub>1.2</sub>C<sub>1.5</sub>Ni<sub>3-x</sub>Mn<sub>x</sub> ( $x=0-0.05$ ) were investigated. Powder samples were prepared by solid state reaction following the method reported by Ren *et al.*<sup>12</sup> for  $x=0$ . The starting materials used were powders of Mg (99.8%, Alfa Aesar), Ni (99.99%, Aldrich) glassy Carbon (Alfa Aesar), and Mn (99.99%, Alfa Aesar). Stoichiometric amounts of these materials were mixed together, pressed into a pellet and sealed in a Ta tube under high purity Argon. Excess of Mg was used to compensate for the volatility of Mg and excess of C was found necessary to arrive at samples with highest  $T_C$ . The mixtures were slowly heated to 600°C and kept for

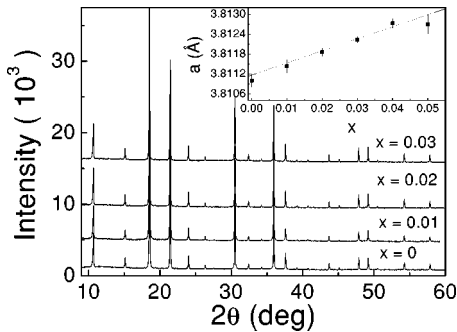


FIG. 1. X-ray diffraction patterns ( $\lambda=0.70930 \text{ \AA}$ ) of  $\text{MgCNi}_{3-x}\text{Mn}_x$  ( $x=0, 0.01, 0.02, 0.03$ ). The patterns are shifted vertically for clarity. The inset shows the variation of the lattice constant  $a$  with concentration.

2 h and heated to  $950^\circ\text{C}$  and again kept for 2 h. After cooling, the pellets were reground and repeatedly annealed at  $950^\circ\text{C}$  for 5 h. X-ray patterns were recorded with Mo radiation ( $\lambda=0.70930 \text{ \AA}$ ) on a Stoe powder diffractometer. dc magnetization measurements were carried out in a MPMS SQUID magnetometer (Quantum Design). ac resistivity measurements ( $\nu=19 \text{ Hz}$ ) were done in a PPMS (Quantum Design) on *in situ* pressed pellets using a home built sapphire cell with Pt contacts employing the van der Pauw method. Specific heat measurements were carried out in the PPMS on powdered samples mixed with Apiezon grease. Addenda from the platform and the grease as determined from separate runs were subtracted.

### III. RESULTS AND DISCUSSION

Figure 1 shows typical x-ray diffraction patterns of some of our samples. All the samples are isostructural. Negligibly small impurity reflections from MgO were observed ( $2\theta \approx 19^\circ$ ). The presence of a minute amount of unreacted Ni is inferred from the observation of a small kink at  $\sim 625 \text{ K}$  in the high-field susceptibility data, coinciding with the Curie temperature of Ni. The lattice parameter of the parent compound ( $x=0$ ) is  $3.8110(2) \text{ \AA}$ . Comparing this value with the reported variation of  $T_C$  versus carbon concentration,<sup>10</sup> we estimate that the carbon content in this sample is  $\sim 0.97$ . The slightly lower carbon concentration results in a reduction of  $T_C$  from the optimal value. With addition of Mn ( $x \neq 0$ ) the cell constant increases as shown in the inset of Fig. 1. The increase in the cell parameters with addition of Mn is consistent with the larger atomic radii of Mn as compared to Ni. We note that in case of Co and Fe doping, very little or no change in cell parameters had been observed.<sup>22</sup>

The variation of the susceptibility as a function of temperature for  $x=0$  and  $0.01$  is shown in Fig. 2. The parent compound ( $x=0$ ) shows a  $T_C^{\text{onset}}$  of  $\approx 6.6 \text{ K}$ . It exhibits a fairly sharp transition and below  $4 \text{ K}$  reaches approximately 100% of the superconducting volume fraction. On substituting Ni with Mn, even for the lowest concentration  $x=0.01$  (0.3 at.% Mn), superconductivity is completely suppressed. A very weak diamagnetic signal was observed at  $1.8 \text{ K}$  which correlates with resistivity data discussed later. For

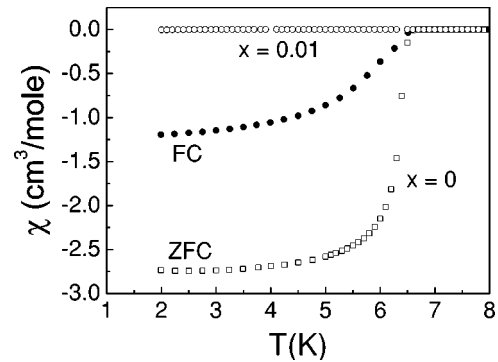


FIG. 2. Magnetic susceptibility  $\chi$  as a function of temperature measured in magnetic field  $H=6 \text{ Oe}$  for samples  $\text{MgCNi}_{3-x}\text{Mn}_x$  ( $x=0, 0.01$ ). Zero-field-cooled (ZFC) and field-cooled (FC) branches are marked.

higher Mn concentration no evidence of superconductivity was found. Additionally, ac susceptibility measurements were carried out down to  $0.3 \text{ K}$  which gave no evidence of superconducting and/or magnetic ordering in Mn doped samples. This rapid suppression of both  $T_C$  ( $\sim -21 \text{ K/at.}\%$  Mn) and volume fraction, on addition of Mn is very different from that reported in the case of Co, Fe, and Cu substitutions, where only a marginal decrease in  $T_C$  had been observed. Substitution of Mn in  $\text{YNi}_2\text{B}_2\text{C}$  also leads to only a marginal decrease of  $0.7 \text{ K/at.}\%$  of Mn.<sup>24</sup> The suppression of superconductivity in Mn doped  $\text{MgCNi}_3$  can be attributed to the formation of local moments the evidence of which comes from paramagnetic susceptibility and resistivity measurements described in the following.

The paramagnetic susceptibility,  $\chi$  as a function of temperature measured in a field of  $1 \text{ kOe}$  is shown in Fig. 3. For  $x=0$  the variation is nearly temperature independent. The magnitude of  $\chi \sim 3.5 \times 10^{-4} \text{ cm}^3/\text{mole}$  is close to that reported by Hayward *et al.*<sup>21</sup> For samples with  $x > 0$  a large increase in  $\chi$  at low temperatures is observed. The temperature dependence of  $\chi$  follows a Curie-Weiss-like behavior and has been fitted to a relation of the form  $\chi = \chi_0 + C/(T - \theta)$  in the temperature range  $5\text{--}300 \text{ K}$ .  $\chi_0 \sim 4 \times 10^{-4} \text{ cm}^3/\text{mole}$  represents the sum of all temperature

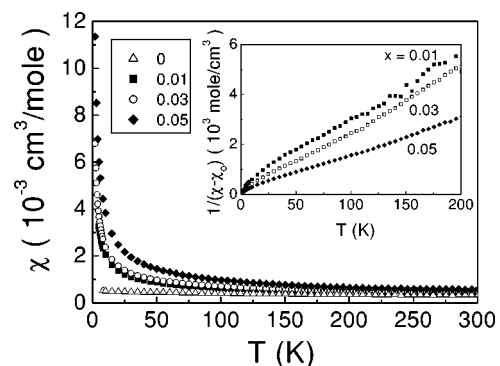


FIG. 3. The normal state magnetic susceptibility  $\chi$  as a function of temperature measured in magnetic field  $H=1000 \text{ Oe}$  for samples  $\text{MgCNi}_{3-x}\text{Mn}_x$  ( $x=0, 0.01, 0.03, 0.05$ ). The inset shows temperature variation of inverse susceptibility for  $x=0.01, 0.03$ , and  $0.05$ .

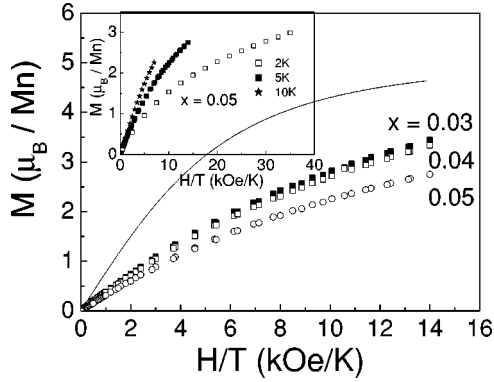


FIG. 4. Magnetization as a function of field of  $\text{MgCNi}_{3-x}\text{Mn}_x$  ( $x=0.03, 0.04, 0.05$ ) at 5 K. The continuous line is the expected variation from a Brillouin function for spin  $S=5/2$ . The inset shows the variation of magnetization with field at temperatures 2, 5, and 10 K for  $x=0.05$ .

independent contributions. The value of  $\theta$  are  $\sim 4$  K. From the Curie constant,  $C$  the paramagnetic moment is estimated. The effective magnetic moment per Mn obtained ( $\sim 6\mu_B$ ) is close to the expected free ion value  $5.9\mu_B$  for  $\text{Mn}^{2+}$  ( $S=5/2$ ). The slight discrepancy results from the uncertainty in the final composition. This is the first report of observation of Curie-Weiss behavior and therefore of a local moment formation in these samples. The field dependence of magnetization at 5 K for samples  $x=0.03, 0.04$ , and  $0.05$  is shown in Fig. 4. There is no hysteresis observed for any composition or temperature. The variation of magnetization is non linear but does not exhibit saturation and does not approach the free ion value expected for  $S=5/2$ . For comparison the expected behavior for  $S=5/2$  is also plotted. Magnetization as a function of magnetic field measured at 2, 5, and 10 K is shown in inset of Fig. 4 for a typical sample  $x=0.05$ . The data at different temperatures do not collapse into a single curve indicating that the doped Mn moments are magnetically interacting.

Indications for a Kondo behavior and associated spin fluctuation effects are observed in the temperature dependence of the resistivity. Figure 5 shows the plot of normalized resistance  $r [=R(T)/R(300\text{ K})]$  as a function of temperature. The resistance decreases with temperature and exhibit a metallic behavior. While the undoped compound shows superconductivity below  $\sim 6.8$  K, the Mn containing compounds exhibit a minimum in  $r(T)$  at  $T_{\min}$ , below which  $r$  increases again with lowering of  $T$ . The residual resistivity ratio (RRR)  $\sim 1.8$  for  $x=0$  is about the same as reported by Waelte *et al.*<sup>21</sup> but lower than that reported by Kumary *et al.*<sup>22</sup> The low value of RRR along with low value of  $T_C$  and cell parameters correlate with the deficiency of carbon. The absolute value of the resistivity in our samples are between  $\sim 10$ – $20$  m $\Omega$  cm which are about an order of magnitude larger than found by others.<sup>21,22</sup> We attribute this difference to grain boundary resistance in the nonsintered pellets used in the experiment. The temperature dependence of  $r$  between 50 and 200 K could be described by the relation

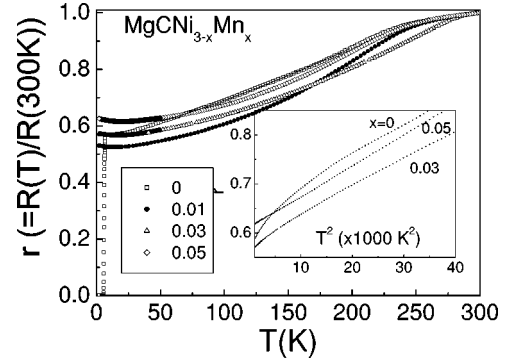


FIG. 5. The variation of normalized resistance  $r [=R(T)/R(300\text{ K})]$  with temperature for samples  $\text{MgCNi}_{3-x}\text{Mn}_x$  ( $x=0, 0.01, 0.03, 0.05$ ). The continuous line through the data points of  $x=0$  is the fit to Eq. (1) (described in the text). The inset shows the  $T^2$  dependence of  $r$  followed in the case of  $x=0, 0.03$ , and  $0.05$ .

$$r(T) = A + BT^2 + C \left( \frac{T}{\theta} \right)^5 \int_0^{\theta/T} dx \frac{x^5}{[(e^x - 1)(1 - e^{-x})]} \quad (1)$$

where  $A$  is a temperature independent term, the second term arises from spin fluctuation effects and the third is the Bloch Grüneisen function. It gives a reasonably good fit to the data. For  $x=0$ , the value of  $\theta_D \sim 238$  K extracted from the fit is slightly lower than that obtained from specific heat measurements  $\theta_D \sim 280$  K. In the Mn containing samples an increase in the coefficient of the  $T^2$  term from  $2.6 \times 10^{-6}$  for  $x=0$  to  $\sim 6.5 \times 10^{-6}$  ( $\text{K}^{-2}$ ) for  $x=0.05$  is observed. The  $T^2$  dependence is shown in the inset of Fig. 5. The enhancement of the  $T^2$  term in  $x \neq 0$  is attributed to an increase in scattering from spin fluctuations.<sup>25</sup>

For samples with  $x \neq 0$  the position of the resistivity minimum  $T_{\min}$  increases from  $\sim 16$  K for  $x=0.01$  to  $\sim 20$  K for  $x=0.05$ , as shown in Fig. 6. And similarly, the depth of the minimum  $[r(1.8\text{ K}) - r(T_{\min})]/r(T_{\min})$  increases from  $\sim 0.8\%$  for  $x=0.01$  to  $\sim 1.7\%$  for  $x=0.05$ . The temperature dependence of  $r(T)$  below  $T_{\min}$  follows a  $-\ln T$  behavior in all the cases. The slope  $1/cdr/d \ln T$  decreases from  $9 \times 10^{-3}$  for  $x=0.01$  to  $2.7 \times 10^{-3}$  ( $\text{K at. \%})^{-1}$  for  $x=0.05$ .

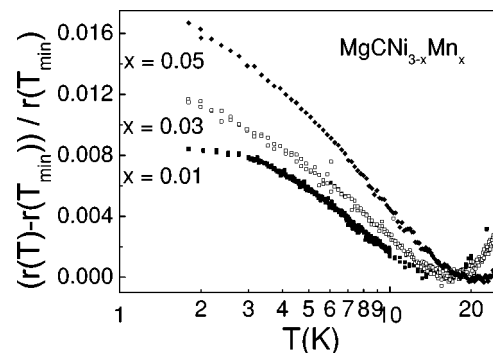


FIG. 6. The variation of  $[r(T) - r(T_{\min})]/r(T_{\min})$  with temperature for samples  $\text{MgCNi}_{3-x}\text{Mn}_x$  ( $x=0.01, 0.03, 0.05$ ) in the region below  $T_{\min}$ .

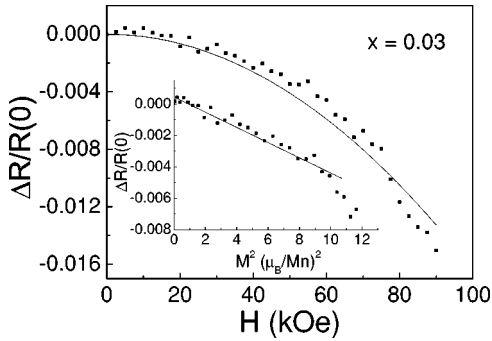


FIG. 7. The variation of magnetoresistance  $\Delta R/R(0)$  with field at  $T=2$  K for  $\text{MgCNi}_{2.97}\text{Mn}_{0.03}$ . The continuous line shows the  $\sim H^2$  dependence. The inset shows the variation of  $\Delta R/R(0)$  with  $M^2$ .

All these features are consistent and indicate a dominating role of Kondo effect<sup>26,27</sup> in the low temperature electronic properties of these samples. The variation of the slope with concentration suggests that the impurities are not isolated but magnetically interacting which supports the conclusion drawn from  $M(H)$  curves. Evidence for a Kondo effect is also found from magnetoresistance (MR) measurements displayed in Fig. 7. The MR  $\Delta R/R(0) = [R(H) - R(0)]/R(0)$  as a function of field is negative and follows a  $\sim H^2$  dependence. The negative MR results from partial alignment of impurity spins which reduces the spin flip scattering. A correlation between the MR and magnetization in a Kondo system has been shown to exist and described by the expression<sup>28,29</sup>

$$\Delta R = R(H, T) - R(0, T) = \frac{3\pi}{2E_F} \frac{m}{e^2\hbar} c V J^2 M^2, \quad (2)$$

where  $m$  and  $e$  are the charge and mass of the electron,  $V$  is the atomic volume,  $J$  the  $s-d$  exchange constant,  $c$  the atomic concentration of impurities,  $E_F$  the Fermi energy, and  $M$  is the magnetization in  $\mu_B/\text{atom}$ . In the inset of Fig. 7 we show such a correlation to exist in these samples. Using  $v_F = 1.5 \times 10^7 \text{ cm}^2/\text{s}$ <sup>16</sup> in the above expression we obtain the value for  $|J| \sim 0.1 \text{ eV}$ . This value of  $J$  is comparable to those reported in the case of dilute alloys of Mn in Cu (Ref. 29) and Mn in PdSb.<sup>30</sup>

Specific heat measurements were carried out in the temperature range 1.8 to 20 K. The data could be fitted (for  $x=0$ , in the range  $T > T_C$ ) to an expression of the form

$$C_p(T) = \gamma T + C_L + C_E + C_{\text{Sch}}, \quad (3)$$

where  $\gamma$  is the Sommerfeld constant,  $C_L$ ,  $C_E$ , and  $C_{\text{Sch}}$  are the Debye, Einstein, and a Schottky term for magnetic contribution, respectively. The Einstein term takes into account the 13 meV octahedral rotational mode.<sup>7</sup> The fitted parameters are shown in Table I. The variation of  $C_p$  with temperature for  $x=0$  is shown in inset of Fig. 8. The superconducting anomaly at  $\sim 7$  K indicates bulk superconductivity and is in agreement with preceding measurements. However, the anomaly in comparison to those reported in the literature<sup>16,19</sup> is somewhat broader possibly indicating a distribution of  $T_C$

TABLE I. Parameters Debye temperature ( $\theta_D$ ), Sommerfeld parameter ( $\gamma$ ), Einstein temperature ( $\theta_E$ ), and Schottky energy ( $\delta_{\text{Schottky}}$ ) obtained from fitting  $C_p(T)$  data to Eq. (3) for samples  $\text{MgCNi}_{3-x}\text{Mn}_x$  ( $x=0, 0.01, 0.03, 0.05$ )

$x$	$\theta_D$ (K)	$\gamma$ (mJ/mole K <sup>2</sup> )	$\theta_E$ (K)	$\delta_{\text{Schottky}}$ (K)
0.0	256	32.0	149	
0.01	288	28.2	150	0.8
0.03	294	32.4	153	1.0
0.05	296	35.0	164	1.6

due to defects. The value of  $\gamma \sim 10.7$  (mJ/mole K per Ni atom) obtained from the fit of the zero field data is in good agreement with other reports in the literature. The absence of superconductivity in  $x \neq 0$  is also evident from specific heat measurements confirming the bulk nature of the effect. The temperature variation of  $C_p$  is shown in Fig. 8 for a typical sample  $x=0.03$ . At low temperatures the increase observed in  $C_p/T$  versus  $T^2$  plot arises from the Schottky anomaly. The maximum is estimated to be at 0.4 K and the energy splitting is  $\sim 1$  K. The values of  $\gamma$  appear to increase (beyond the uncertainty of fitting) with increasing Mn concentration. This observation indicates conclusively that reduction in  $T_C$  with addition of Mn is due to the pair breaking interaction which is of magnetic origin and not electronic. Similar studies of specific heat in carbon deficient samples show that the reduction in  $T_C$  correlate with the decrease in  $\gamma$ .<sup>11</sup> On application of magnetic field, the maximum in the Schottky anomaly shifts to higher temperatures. Inset (b) in Fig. 8 shows the difference plot,  $C_p(90 \text{ kOe}) - C_p(0 \text{ kOe})$  versus  $T$  for a sample with  $x=0.03$ . A broad maximum is observed at  $\sim 9$  K. Qualitatively, the nature of the curve could be reproduced by assuming a Schottky anomaly for a two level system. The excess specific heat on application of field is understood to arise from the removal of the degeneracy of the Kondo quasibound state. The entropy obtained is within 25% of the expected value ( $R \ln 2$ ) for  $S=1/2$ .

From susceptibility measurements the Kondo temperature  $T_K$  was estimated using the expression  $\chi(T) = g^2 \mu_B^2 S(S$

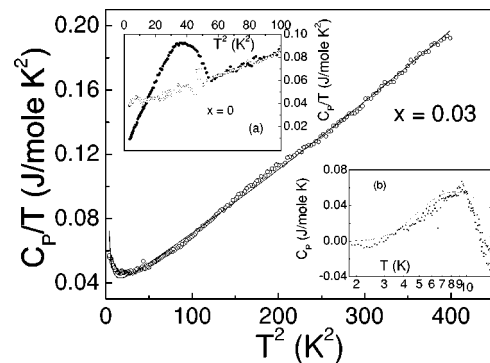


FIG. 8. The plot of  $C_p/T$  versus  $T^2$  for  $\text{MgCNi}_{2.97}\text{Mn}_{0.03}$ . The continuous line is the fit to Eq. (3). In the inset (a) is shown the variation of  $C_p/T$  versus  $T^2$  for  $\text{MgCNi}_3$  ( $\bullet H=0$ ,  $\circ H=90 \text{ kOe}$ ). In the inset (b) is shown the difference  $C_p(H=90 \text{ kOe}) - C_p(H=0)$  against  $T$  for  $\text{MgCNi}_{2.97}\text{Mn}_{0.03}$ . The solid curve is generated assuming a two level Schottky effect.



+1)/3.66( $k_B T + 4.5 T_K$ ) (Ref. 26) valid for  $T > T_K$ . Comparing the  $\theta$  values we find  $T_K \sim 1$  K in these compositions. It is of interest to note that we also find that  $T_C$  is only marginally reduced to 5.5 K in the case of  $\text{MgCNi}_{2.95}\text{V}_{0.05}$  and  $\text{MgCNi}_{2.95}\text{Cr}_{0.05}$ . In addition, no Curie-Weiss behavior is observed. The absence of moment in the case of Cr and V doped samples is contrary to the results arrived at by electronic structure calculations by Granada *et al.*,<sup>20</sup> where it is shown that moments are formed more easily as the difference in atomic number  $\Delta Z$  between Ni and transition metal increases. Therefore, we conclude local moments form only in the case of Mn and they greatly inhibit superconductivity. The reduction of  $T_C$  in the presence of paramagnetic impurities has been worked out by Abrikosov and Gorkov (AG).<sup>31</sup> Within the AG theory the variation of  $T_C$  is given by the relation

$$\ln \frac{T_C}{T_{C0}} = \psi\left(\frac{1}{2}\right) - \psi\left(\frac{1}{2} + \rho\right), \quad (4)$$

where  $T_{C0} = T_C$  for  $x=0$ ,  $\psi$  is the digamma function, and  $\rho (= \alpha/2\pi k_B T_C)$  contains  $\alpha$ , the pair breaking energy. In terms of  $J$  and  $S$ ,  $\alpha$  is expressed as  $\alpha = 4\pi c N(E_F) J^2 S(S+1)$ . Müller-Hartmann and Zittartz (MZ)<sup>32</sup> in their theory on the effect of Kondo behavior on superconductivity have shown that the variation of  $T_C$  with concentration is markedly different from the AG theory. In this case the pair breaking strength depends upon  $T_C$  and  $\rho$  is expressed as

$$\rho = c \frac{T_{C0}}{T_C} \frac{\pi^2 S(S+1)}{\ln^2 T_C / T_K + \pi^2 S(S+1)}. \quad (5)$$

As a result, the reduction of  $T_C$  with impurity concentration is a function of  $T_K/T_C$ . For the case,  $T_K \ll T_C$  a characteristic reentrant superconducting-normal behavior is observed.<sup>33</sup> In Fig. 9 we plot the variation of  $T_C$  with normalized concentration  $\bar{c} = c/(2\pi)^2 N(E_F) T_C$  for the case of  $S=5/2$  using the estimated values of  $J$  and  $T_K$  for  $\text{MgCNi}_3$  in the expressions from AG and MZ theory. In the presence of Kondo effect the suppression of  $T_C$  is much more rapid than in the case of normal paramagnetic impurities. The critical concentration as observed in the figure  $\bar{c}=0.15$  ( $\approx 0.35$  at. %) is in good agreement with our observation of absence of superconductivity in samples with 0.3 at. % Mn. Electronic structure calculations for  $\text{MgCNi}_3$  estimate the moment on doped Co atoms to be  $\sim 10^{-5} \mu_B/\text{atom}$  and attribute the suppression of superconductivity to spin fluctuations and strong  $d-d$  covalent interactions. Similar calcula-

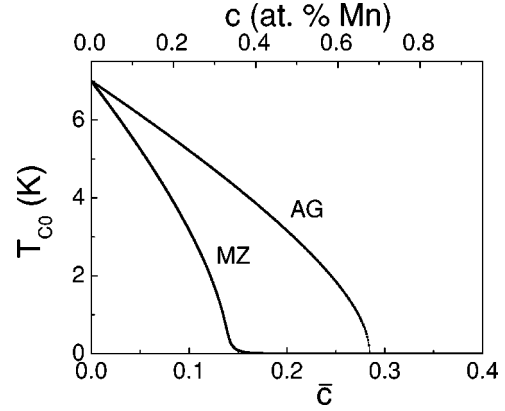


FIG. 9. The plot of  $T_C$  versus normalized concentration  $\bar{c}$  [ $= c/(2\pi)^2 N(E_F) T_C$ ] for the case of  $S=5/2$  using the estimated values of  $J$  and  $T_K$  in the expressions from AG and MZ theory.

tions have been reported for the case of Mn substitution with  $x=0.042$  and show that Mn forms a magnetic moment of  $1.06 \mu_B$ .<sup>19</sup> As against Co, the rapid suppression of  $T_C$  in Mn is ascribed to the overlap of the Mn  $d$  states with the majority band of Ni states. The systematic decrease in the value of  $R(300 \text{ K})/R(T_{\min})$  with increase in Mn concentration indicates that the virtual bound states which form with Mn doping are close to  $E_F$ . Such enhanced pair breaking effects on introduction of Mn in contrast to other transition metals have been observed earlier in case of TM-Al alloys.<sup>34</sup> We believe that Coulomb repulsion, occupation number of  $d$  electrons and Kondo effect play a role in suppressing superconductivity on substituting Ni with other transition metals in  $\text{MgCNi}_3$ .

#### IV. CONCLUSION

In summary, we show that partially substituting Ni with Mn dramatically alters superconductivity in  $\text{MgCNi}_3$  as compared to substitution of Ni with other transition metals. Doping by as little as 0.3 at. % of Mn completely suppresses superconductivity. The Mn containing samples exhibit Curie-Weiss behavior in temperature dependence of susceptibility and Kondo effect which leads to rapid suppression of superconductivity.

#### ACKNOWLEDGMENTS

We thank Eva Bruecher and Gisela Siegle for their assistance in carrying out the various measurements. One of us (A.D.) acknowledges the Max-Planck Society for financial support.

\*On leave from Solid State Physics Division, Bhabha Atomic Research Center, Mumbai 400 085, India; Electronic address: adas@apsara.barc.ernet.in

<sup>1</sup>T. He, Q. Huang, A.P. Ramirez, Y. Wang, K.A. Regan, N. Rogado, M.A. Hayward, M.K. Haas, J.J. Slusky, K. Inumara, H.W. Zandbergen, N.P. Ong, and R.J. Cava, *Nature (London)* **411**, 54 (2001).

<sup>2</sup>R. Nagarajan, C. Mazumdar, Z. Hossain, S.K. Dhar, K.V. Go-

palakrishnan, L.C. Gupta, C. Godart, P.D. Padalia, and R. Vijaraghavan, *Phys. Rev. Lett.* **72**, 274 (1994).

<sup>3</sup>R.J. Cava, H. Takagi, H.W. Zandbergen, J.J. Krajewski, W.F. Peck, Jr., T. Siegrist, B. Batlogg, R.B. van Dover, R.J. Felder, K. Mizuhashi, J.C. Lee, H.E. Isoki, and S. Uchida, *Nature (London)* **367**, 252 (1994).

<sup>4</sup>H. Prozorov, A. Snezhko, T. He, and R.J. Cava, cond-mat/0302431(v1) (unpublished).

- <sup>5</sup>A. Szajek, *J. Phys.: Condens. Matter* **13**, L595 (2001).
- <sup>6</sup>S.B. Dugdale and T. Jarlborg, *Phys. Rev. B* **64**, 100508 (2001).
- <sup>7</sup>D. Singh and I. Mazin, *Phys. Rev. B* **64**, 140507 (2001).
- <sup>8</sup>J.H. Shim, S.K. Kwon, and R.I. Min, *Phys. Rev. B* **64**, 180510 (2001).
- <sup>9</sup>H. Rosner, R. Weht, M.D. Johannes, W.E. Pickett, and E. Tossatti, *Phys. Rev. Lett.* **88**, 027001 (2002).
- <sup>10</sup>T.G. Amos, Q. Huang, J.W. Lynn T. He, and R.J. Cava, *Solid State Commun.* **121**, 73 (2002).
- <sup>11</sup>L. Shan, K. Xia, Z.Y. Lin, H.H. Wen, Z.A. Ren, G.C. Che, and Z.X. Zhao, *cond-mat/0302116* (unpublished).
- <sup>12</sup>Z.A. Ren, G.C. Che, S.L. Jia, H. Chen, Y.M. Ni, G.D. Lin, and Z.X. Zhao, *Physica C* **371**, 1 (2002).
- <sup>13</sup>S.Y. Li, R. Fan, H.H. Chen, C.H. Wang, W.Q. Mo, K.Q. Ruan, Y.M. Xiong, X.G. Luo, H.T. Zhang, L. Li, Z. Sun, and L.Z. Cao, *Phys. Rev. B* **64**, 132505 (2001).
- <sup>14</sup>J.-Y. Lin, p.L. Ho, H.L. Huang, p.H. Lin, Y.-L. Zhang, R.-C. Yu, C.-Q. Jin, and H.D. Yang, *cond-mat/0202034* (unpublished).
- <sup>15</sup>Z.Q. Mao, M.M. Rosario, K.D. Nelson, K. Wu, I.G. Deac, p. Schiffer, and Y. Liu, *cond-mat/0105280(v3)* (unpublished).
- <sup>16</sup>A. Wälte, H. Rosner, M.D. Johannes, G. Fuchs, K.-H. Müller, A. Handstein, K. Nenkov, V.N. Narozhnyi, S.-L. Drechsler, S. Shulga, and L. Schultz, *cond-mat/0208364* (unpublished).
- <sup>17</sup>P.M. Singer, T. Imai, T. He, M.A. Hayward, and R. J. Cava, *Phys. Rev. Lett.* **87**, 257601 (2001).
- <sup>18</sup>In Gee Kim, Jae Il Lee, and A.J. Freeman, *Phys. Rev. B* **65**, 064525 (2002).
- <sup>19</sup>J.L. Wang, Y. Xu, Z. Zeng, Q.Q. Zheng, and H.Q. Lin, *J. Appl. Phys.* **91**, 8504 (2002).
- <sup>20</sup>C.M. Granada, C.M. de Silva, and A.A. Gomes, *Solid State Commun.* **122**, 269 (2002).
- <sup>21</sup>M.A. Hayward, M.K. Haas, A.p. Ramirez, T. He, K.A. Regan, N. Rogado, K. Inumaru, and R.J. Cava, *Solid State Commun.* **119**, 491 (2001).
- <sup>22</sup>T.G. Kumary, J. Janaki, Awadesh Mani, S. Mathi Jaya, V.S. Sasstry, Y. Hariharan, T.S. Radhakrishnan, and M.C. Valsakumar, *Phys. Rev. B* **66**, 064510 (2002).
- <sup>23</sup>Z.A. Ren, G.C. Che, S.L. Jia, H. Chen, Y.M. Ni, and Z.X. Zhao, *cond-mat/0105366* (unpublished).
- <sup>24</sup>F.S. da Rocha, G.L.F. Fraga, D.E. Brandao, and A.A. Gomes, *Physica C* **363**, 41 (2001).
- <sup>25</sup>J. Dugdale, *The Electrical Properties of Metals and Alloys* (Edward Arnold, London, 1977).
- <sup>26</sup>A. Heeger, *Solid State Physics* (Academic Press, New York, 1969), Vol. 23, p. 283.
- <sup>27</sup>M. D. Daybell, *Magnetism* (Academic Press, New York, 1973), Vol. V, p. 121.
- <sup>28</sup>M.-T. Béal-Monod and R. Weiner, *Phys. Rev.* **552**, 170 (1968).
- <sup>29</sup>P. Monod, *Phys. Rev. Lett.* **19**, 1113 (1967).
- <sup>30</sup>T.H. Geballe, B.T. Matthias, B. Caroli, E. Corenzwit, J.p. Maita, and G.W. Hull, *Phys. Rev.* **169**, 457 (1968).
- <sup>31</sup>A. Abrikosov and L. Gor'kov, *Sov. Phys. JETP* **12**, 1243 (1961).
- <sup>32</sup>E. Müller-Hartmann and J. Zittartz, *Phys. Rev. Lett.* **26**, 428 (1971).
- <sup>33</sup>M.W.A. Fertig, A.C. Mota, L.E. DeLong, D. Wohlleben, and R. Fitzgerald, *Solid State Commun.* **11**, 829 (1972).
- <sup>34</sup>E. K. S. M. Vonsovsky and Yu. A. Izynmov, *Superconductivity of Transition Metals*, Vol. 27 of *Springer Series in Solid-State Sciences* (Springer-Verlag, Berlin, 1982).